Pergamon

Geochimica et Cosmochimica Acta, Vol. 67, No. 3, pp. 473–485, 2003

0016-7037/03 $22.00 + .00

PII S0016-7037(02)01139-0

The influence of pressure and composition on the viscosity of andesitic melts

CHRISTIAN LIEBSKE,[1,2,*] HARALD BEHRENS,[1] FRANÇOIS HOLTZ,[1] and REBECCA A. LANGE[2]

[1]Institut für Mineralogie, Universität Hannover, Welfengarten 1, 30167 Hannover, Germany
[2]Department of Geological Science, 2534 C.C. Little Building, University of Michigan, Ann Arbor, MI 48109-1063, USA

(*Received January* 8, 2002; *accepted in revised form July* 31, 2002)

Abstract—The effect of pressure and composition on the viscosity of both anhydrous and hydrous andesitic melts was studied in the viscosity range of 10^8 to $10^{11.5}$ Pa · s using parallel plate viscometry. The pressure dependence of the viscosity of three synthetic, iron-free liquids (andesite analogs) containing 0.0, 1.06, and 1.96 wt.% H_2O, respectively, was measured from 100 to 300 MPa using a high-*P*-*T* viscometer. These results, combined with those from Richet et al. (1996), indicate that viscosities of anhydrous andesitic melts are independent of pressure, whereas viscosities of hydrous melts slightly increase with increasing pressure. This trend is consistent with an increased degree of depolymerization in the hydrous melts. Compositional effects on the viscosity were studied by comparing iron-free and iron-bearing compositions with similar degrees of depolymerization. During experiments at atmospheric and at elevated pressures (100 to 300 MPa), the viscosity of iron-bearing anhydrous melts preequilibrated in air continuously increased, and the samples became paramagnetic. Analysis of these samples by transmission electron microscopy showed a homogeneous distribution of crystals (probably magnetite) with sizes in the range of 10 to 50 nm. No significant difference in the volume fractions of crystals was found in samples after annealing for 170 to 830 min at temperatures ranging from 970 to 1122 K. An iron-bearing andesite containing 1.88 wt.% H_2O, which was synthesized at intrinsic fO_2 conditions in an internally heated pressure vessel, showed a similar viscosity behavior as the anhydrous melts. The continuous increase in viscosity at a constant temperature is attributed to changes of the melt structure due to exsolution of iron-rich phases. By extrapolating the time evolution of viscosity down to the time at which the run temperature was reached, for both the anhydrous (at 1055 K) and the hydrous (at 860 K) iron-bearing andesite, the viscosity is 0.7 log units lower than predicted by the model of Richet et al. (1996). This may be explained by differences in structural properties of Fe^{2+} and Fe^{3+} and their substitutes Mg^{2+}, Ca^{2+}, and Al^{3+}, which were used in the analogue composition.

The effect of iron redox state on the viscosity of anhydrous, synthetic andesite melts was studied at ambient pressure using a dilatometer. Reduced iron-bearing samples were produced by annealing melts in graphite crucibles in an Ar/CO atmosphere for different run times. In contrast to the oxidized sample, no variation of viscosity with time and no exsolution of iron oxide phases was observed for the most reduced glasses. This indicates that trivalent iron promotes the exsolution of iron oxide in supercooled melts. With decreasing $Fe^{3+}/\Sigma Fe$ ratio from 0.58 to 0.34, the viscosity decreases by ~1.6 log units in the investigated temperature range between 964 and 1098 K. A more reduced glass with $Fe^{3+}/\Sigma Fe = 0.21$ showed no additional decrease in viscosity. Our conclusion from these results is that the viscosity of natural melts may be largely overestimated when using data obtained from samples synthesized in air. *Copyright © 2003 Elsevier Science Ltd*

1. INTRODUCTION

The viscosity of igneous melts is one of the most important physical properties controlling the evolution of magmatic systems. The viscosity greatly influences processes such as the ascent of melts in the Earth's mantle and crust, differentiation processes in magma chambers, and the behavior of volcanic eruptions. Hence, there is a fundamental interest in geoscience in predicting viscosities of magmatic systems at various conditions.

To establish a viscosity model applicable to various geological situations, the melt viscosity must be known over a wide range of temperatures. Experimental data can be obtained at high temperatures above the liquidus (viscosities of $\eta \leq 10^5$ Pa · s) and at low temperatures near the glass transition (viscosities of $\eta \geq 10^8$ Pa · s). Between both temperature regions, crystallization of the samples prohibits experimental determination of viscosities.

In the high-temperature range at ambient pressure, the concentric cylinder method is well suited to determine viscosities of anhydrous samples (e.g., Scarfe et al., 1983; Dingwell, 1986). High pressures are required to study melts containing volatiles in the low-viscosity range because of their low solubility at atmospheric pressure. Experiments can be realized by using the falling sphere method developed by Shaw (1963). This technique also allows the pressure dependence of viscosities to be quantified (e.g., Kushiro et al., 1976; Dingwell and Mysen, 1985; Scarfe et al., 1987).

In the glass transition range, several techniques have been applied to investigate the influence of various parameters on the rheology of silicate melts. For example, Webb and Dingwell (1990) investigated stress-strain relationships with the fiber-elongation method, and Lejeune and Richet (1995) used the parallel-plate technique to determine viscosities of melts containing a defined crystal fraction. Water-bearing compositions

* Author to whom correspondence should be addressed, at Bayerisches Geoinstitut, Universität Bayreuth, 95440 Bayreuth, Germany (christian.liebske@uni-bayreuth.de).

can be investigated in the high-viscosity range at ambient pressure because of slow dehydration kinetics. Dingwell et al. (1996) studied a polymerized granitic melt with H_2O contents between 0.4 and 3.5 wt.%, Richet et al. (1996) and Whittington et al. (2001) examined melts with intermediate polymerization (0 to 4.92 wt.% H_2O), and Whittington et al. (2000) studied strongly depolymerized melts (0 to 5 wt.% H_2O). To our knowledge, the only studies on the pressure dependence of viscosity in this temperature range were performed by Schulze et al. (1999) and Schulze (2000) using a parallel plate viscometer incorporated in an internally heated pressure vessel (IHPV).

Few data exist concerning the influence of iron and its redox state on the viscosity of geologically relevant silicate melts. At superliquidus temperatures, Dingwell and Virgo (1987) and Dingwell (1989, 1991) studied the dependence of melt viscosity on the oxidation state of iron in iron-bearing alkali and alkaline-earth systems. The viscosity of slags was investigated by Toguri et al. (1976) and Seki and Oeters (1984). Moreover, studies by Urbain et al. (1982) and Mysen et al. (1985) dealt with iron-bearing silicate melts. In the glass transition range, Williamson et al. (1968), Cukierman and Uhlmann (1974), Klein et al. (1983), and Montenero et al. (1986) reported a dramatic decrease in viscosity when the melt became more reduced. However, the investigated melts in the superliquidus temperature range as well as in the glass transition range were often simple, synthetic liquids, so that constraints on the effect of iron redox state on melt viscosity are not quantified for magmatic liquids.

In this contribution, we report new experimental data on the viscosity of anhydrous and hydrous andesitic melts at temperatures near the glass transition. To avoid experimental difficulties due to dissolved iron, compositional analogues in which iron was substituted by appropriate amounts of other elements were used in previous viscosity studies (Richet et al., 1996; Whittington et al., 2000, 2001). Disadvantages of this approach are that the binding properties of the substitutes might not be identical to those of the iron species and that the ratio of network former to network modifier is fixed. In natural melts, the $Fe^{3+}/\Sigma Fe$ ratio varies with oxygen fugacity, imposing a change in melt polymerization. We have tested possible effects of element substitution on melt viscosity by comparing viscosity data of iron-free and iron-bearing andesite (anhydrous and hydrous) and by measuring the dependence of the viscosity of iron-bearing melts on the redox state of iron. In addition, we have determined the pressure dependence of viscosity for the iron-free composition to enable application of the viscosity data at elevated pressures.

2. EXPERIMENTAL AND ANALYTICAL METHODS

2.1. Synthesis of Anhydrous Glasses

An andesite from Unzen Volcano (Pre Unzen 500 kyr; Chen et al., 1993) was chosen as the starting composition. To compare the viscosities of an iron-free and an iron-bearing melt, we synthesized an iron-free analog of this andesite. Using the empirical model of Kilinc et al. (1983), the concentration of ferrous iron in the natural composition at the synthesis conditions ($T = 1873$ K , $\log_{10} fO_2 = -0.67$) was calculated to be 3.88 wt.%. To obtain similar structures of the iron-free and the iron-bearing melts, ferrous iron was considered to be a network modifier (e.g., Mysen, 1991) and thus replaced by Ca and Mg, preserving the same Mg/Ca ratio as in the natural andesite. Ferric iron was regarded as a network former, and it was substituted for by Al. To simplify the chemical composition of the iron-free andesitic glass, the elements Ti and Mn were eliminated by keeping the same relative proportions of the major elements.

Table 1. Electron microprobe analysis of the starting material (wt.%).

	Unzen andesite	σ	Iron-free andesite	σ
SiO_2	56.65	0.41	58.69	0.33
TiO_2	1.01	0.04	0.01	0.01
Al_2O_3	17.41	0.15	21.57	0.33
FeO^{tot}	8.16	0.21	0.02	0.03
MnO	0.13	0.04	0.02	0.02
MgO	4.30	0.07	5.38	0.10
CaO	7.38	0.11	9.49	0.18
Na_2O	3.23	0.15	3.30	0.10
K_2O	1.56	0.07	1.57	0.12

All iron is given as FeO.

Anhydrous glasses were synthesized by melting mixtures of oxides and carbonates at 1873 K for 4 h in Pt crucibles in air. To improve the homogeneity, the obtained glasses were ground and remelted for 4 h at the same temperature. The homogeneity and chemical composition of the glasses was confirmed by electron microprobe using a Cameca Camebax with a defocused beam of 15 μm operating at an accelerating voltage of 15 kV and a beam current of 18 nA. The results are given in Table 1.

A part of the iron-bearing anhydrous glass was reduced in graphite containers under an Ar/CO atmosphere at 0.1 MPa. Two or three holes (10 mm in height, 2.5 to 3 mm in diameter) were drilled axially in a graphite rod (10 mm in diameter). The holes were filled with glass powder. The reduction was performed in a Deltech gas-mixing furnace using a Tylan mass flow controller with a gas mixture of 99% Ar and 1% CO. The graphite rod was positioned in a Pt basket that was hung from a Pt wire in the hot spot of the furnace. Under these extremely reducing conditions, metallic iron forms in the melts at thermodynamic equilibrium. Thus, different oxidation states can be achieved only by varying the synthesis duration. Syntheses were quenched by melting the Pt wire. Run durations were between 20 and 180 min at 1573 K. The resulting reduced glass cylinders were typically 4 to 5 mm in height.

2.2. Synthesis of Hydrous Glasses

Hydrous glasses were synthesized by high pressure fusion of H_2O plus glass powder in an IHPV. Known amounts of doubly distilled water were added to a dry glass powder composed of a 1:1 mixture of grain sizes of <200 μm and 200 to 500 μm. Hydrous iron-free samples were synthesized in sealed Pt capsules (6 mm in diameter, 35 mm in length). Iron-bearing compositions were synthesized in $Au_{80}Pd_{20}$ capsules (5 mm in diameter, 35 mm in length) to avoid iron loss to the capsule material. The samples were held for 30 to 72 h at 1523 K and 200 MPa. Iron-free compositions were isobarically quenched at a rate of 100 to 200 K/min by switching off the furnace. To avoid crystallization during cooling, the rapid quench device described by Berndt et al. (2002) was used for iron-bearing samples. The cooling rate was estimated to be $\sim$150 K/s for this equipment using the geospeedometer of Zhang et al. (2000) based on water speciation in rhyolitic glasses. The absence of crystals and bubbles in the glasses was checked by using optical microscopy. Water concentrations were determined by Karl-Fischer titration within a maximum analytical error $\pm$0.10 wt.% H_2O for these samples (see Behrens et al., 1996, for more details).

2.3. Viscosity Measurements

Viscosity measurements under high pressure were performed using the parallel plate viscometer, as described in detail by Schulze et al. (1999). Cylindrical samples ranged between 3 and 4 mm in diameter

Table 2. Viscosity η and fit parameter of anhydrous and hydrous iron-free andesitic melts determined under various pressures.

Dry									1.06 (±0.05) wt.% H_2O						1.96 (±0.06) wt.% H_2O					
100 MPa			200 MPa			300 MPa			200 MPa			300 MPa			100 MPa			300 MPa		
T (K)	log η	No.	T (K)	log η	No.	T (K)	log η	No.	T (K)	log η	No.	T (K)	log η	No.	T (K)	log η	No.	T (K)	log η	No.
1036	11.58	b5	1036	11.32	b4	1081	10.02	a8	917	10.55	5	908	11.03	14	840	10.80	9	835	11.14	8
1054	10.77	b6	1054	10.83	b2	1091	9.72	a9	928	10.44	15	918	10.65	13	849	10.52	10	835	11.33	16
1065	10.45	b7	1062	10.30	a1	1100	9.44	a10	937	10.07	1	938	10.07	7	851	10.43	15	844	10.80	7
1075	10.16	b8	1065	10.44	b3	1110	9.17	a11	935	9.97	6	948	9.81	8	859	10.20	11	853	10.51	6
1084	9.87	b9	1074	10.15	b1	1120	8.91	a12	954	9.54	2	948	9.78	12	870	9.85	14	863	10.17	1
1096	9.55	b10	1083	9.74	a2	1130	8.67	a13	976	9.00	3	957	9.57	9	879	9.57	13	864	10.15	5
1106	9.30	b11	1088	9.63	a3				985	8.74	4	977	9.04	10	889	9.32	12	873	9.86	2
1116	9.06	b12	1094	9.48	a4				996	8.54	16	987	8.77	11				883	9.56	3
			1103	9.25	a5				1013	8.13	17							893	9.27	4
			1113	8.99	a6															
			1123	8.75	a7															
A		–22.81 (1.19)		–22.24 (1.10)			–21.18 (0.56)			–15.63 (0.83)			–16.75 (0.36)			–16.52 (0.36)			–18.89 (0.97)
$B \times 10^{-4}$		3.55 (0.13)		3.47 (0.12)			3.37 (0.06)			2.40 (0.08)			–2.52 (0.04)			2.30 (0.03)			2.51 (0.08)
E_a		679 (25)		665 (23)			645 (12)			460 (15)			482 (7)			439 (6)			480 (16)

No. refers to the sequence of measurement.

and 8 and 10 mm in length. The ends of the cylinders were cut and polished parallel. The accessible viscosity range covers 3 orders of magnitude from $10^{8.5}$ to $10^{11.5}$ Pa · s at a maximum temperature of 1173 K and a maximum pressure of 400 MPa. Determination of the melting point of Zn in every experiment was used for temperature calibration, resulting in an accuracy of ±3 K. The maximum error of viscosity is 0.15 log units. The precision of individual measurements, however, is significantly better (±0.05 log units; Schulze et al., 1999).

Viscosity measurements of the iron-bearing composition at ambient pressure were performed by the parallel plate technique using a Perkin Elmer TMA-7 thermomechanical analyzer. Cylindrical samples were cored from the starting material, which had been equilibrated in air or obtained from the glass reduction technique described above. The dimensions of the cylinders ranged between 2.6 and 3.0 mm in diameter and 3.0 and 3.8 mm in length. The ends of the cylinders were polished parallel to each other. Disks of Au (thickness = 0.08 mm) were attached above and below the sample to protect the silica probe and the silica platform from contamination by the sample material. Two S-type thermocouples ($PtRh_{10}$-Pt) at the top and the bottom of the sample monitored the sample temperature, while a K-type (Ni-NiCr) thermocouple was used to control the furnace. Differences in the temperature at the top and the bottom of the sample were <3 K. During the experiments, a constant force of 1 N was applied to the samples. In the first step, the sample was heated at a rate of 50 K/min to the starting temperature at which the viscosity of the sample was expected to be $\sim 10^9$ Pa · s to equilibrate the apparatus thermally for 10 to 15 min. The temperature was then changed in steps of 5 to 10 K to access the complete range of viscosity. Depending on the rate of the deformation, samples were held at constant temperature between 1 and 10 min. The apparatus was calibrated against National Bureau of Standards 711 lead silica glass. Viscosities of this glass were reproduced within 0.1 log units. Because of the uncertainty in temperature, the absolute error of this method is estimated to be 0.2 log units in viscosity.

Both techniques for viscosity determination are based on the parallel-plate method, and the following equation, presented by Neuville and Richet (1991), was applied to calculate the viscosity η, where σ denotes the applied stress and L is the sample length:

$$\eta = \frac{\sigma}{3 \cdot \left(\frac{\mathrm{d} \ln L}{\mathrm{d}T}\right)}. \quad (1)$$

During measurement, the temperature and the deformation rate ($\mathrm{d}\ln L/\mathrm{d}T$) were stored continuously by an IBM-compatible PC. After all viscosity measurements, samples were checked for regular deformation. Temperature gradients or inhomogeneous distribution of water would lead to an irregular shape of the samples, but this was not observed for any of our samples.

2.4. Additional Analytical Techniques

Before and after viscosity measurements on the iron-bearing samples, the FeO concentration was measured by the microanalytical method of Wilson (1960). The concentration of ferric iron was calculated as the difference between total iron and iron in the ferrous state (Fe_2O_3 wt.% = 1.1113 [FeO^{total}-FeO] wt.%). The 2σ error of this method is 0.21 wt.% FeO and is independent of the ferrous iron concentration (Lange and Carmichael, 1989).

Selected samples used in viscosity measurements were analyzed by a Philips CM12 scanning transmission electron microscope operating at 120 kV. Near-infrared (NIR) spectra were collected with a Bruker IFS88 Fourier-transform infrared (FTIR) spectrometer using a tungsten white light source, a CaF_2 beam splitter, and a HgCdTe detector. Samples were prepared as doubly polished thin sections. A high spatial resolution of 30 μm was achieved using a Bruker A590 IR microscope connected to the FTIR spectrometer. One hundred scans were accumulated for each NIR spectrum.

3. RESULTS

3.1. Viscosities Under High Pressure

Two anhydrous and two hydrous iron-free andesites with 1.06 ± 0.05 wt.% and 1.96 ± 0.06 wt.% H_2O were investigated at pressures from 100 to 300 MPa. Three anhydrous and one hydrous (1.88 ± 0.05 wt.% H_2O) iron-bearing andesite were measured at 200 MPa.

3.1.1. Iron-Free Samples

The viscosities of the anhydrous and hydrous iron-free andesitic melts are presented in Table 2. Two different anhydrous samples were used to cover the whole *P-T* range so that the scatter of the data is larger than for the hydrous samples (Fig. 1). At constant pressure and water content, the viscosity can be described at temperatures near the glass transition by an Arrhenius relationship:

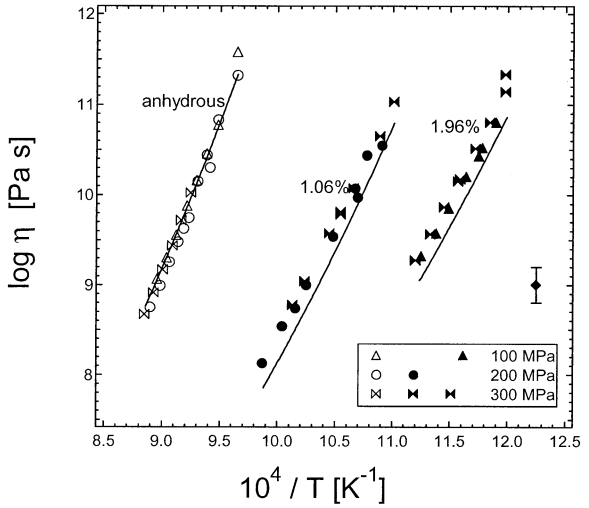

Fig. 1. Viscosities of iron-free andesite melts (anhydrous, 1.06 wt.% H_2O, 1.96 wt.% H_2O) as a function of the reciprocal temperature at different pressures. Solid lines represent calculated values using the model of Richet et al. (1996).

$$\log\eta = A + \frac{B}{T}, \qquad (2)$$

where A and B are fit parameters and T is temperature (K). The activation energy E_a of the viscous flow was calculated from parameter B, with $E_a = B \cdot 2.303 \cdot R$, where R is the gas constant ($R = 8.3144\ \mathrm{J \cdot K^{-1} \cdot mol^{-1}}$). Fit parameters and activation energies are included in Table 2. To investigate the influence of pressure on the viscosity at a constant temperature but different water concentrations, Eqn. 2 was used to calculate viscosities at temperatures at which the model of Richet et al. (1996) predicts viscosities of 10^9, 10^{10}, and 10^{11} Pa · s, respectively (Figs. 2a to 2c). Viscosities of the anhydrous andesite are consistent with the calculations of Richet et al. (1996), although our composition differs slightly from that used by Richet et al. (1996). The maximum deviation of one data point at 200 MPa is 0.22 log units in viscosity, which corresponds to a temperature difference of 7.5 K. Viscosities of hydrous melts are systematically higher than predicted by the model of Richet et al. (1996). The average deviation for the melt containing 1.06 wt.% H_2O is 0.23 log units at 200 MPa and 0.28 log units at 300 MPa. The viscosity deviation for the melt with 1.96 wt.% H_2O is 0.12 and 0.25 log units at 100 MPa and 300 MPa, respectively. After the experiment, a thin slice of the sample with 1.96 wt.% H_2O was cut perpendicular to the long axis of the cylinder to check for water loss by NIR spectroscopy. No variations were observed in the peak heights of the absorption bands at 4500 cm^{-1} and 5200 cm^{-1}, assigned to OH groups and molecular water, respectively. If water gradients were present in the samples, they were restricted to a very small layer (<30 μm) near the surface. On the basis of the absence of measurable water gradients and the reproducibility of measurements during each experiment (see Table 2), we infer that water loss caused no problems in our viscosity measurements.

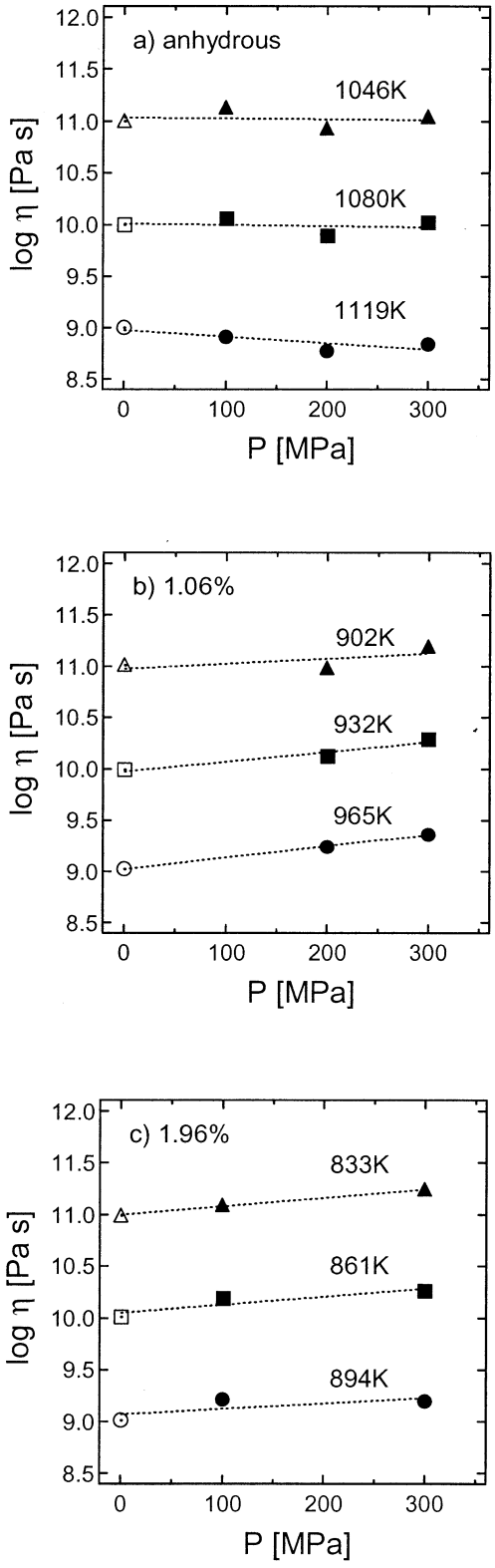

Fig. 2. Isothermal presentation of the pressure dependence of the viscosity of iron-free andesite melts at different reference temperatures. (a) Anhydrous, (b) 1.06 wt.% H_2O, (c) 1.96 wt.% H_2O. Filled symbols refer to data from this study; open symbols are predicted values using the model of Richet et al. (1996).

3.1.2. Iron-Bearing Samples

Two anhydrous iron-bearing samples (AndU0a, AndU0b) were studied at various temperatures near the glass transition. At all conditions, the viscosity continuously increased with time. This is consistent with the viscosity results on andesitic melts of Neuville et al. (1993) and Richet et al. (1996). For a better characterization of the time evolution of the viscosity, two runs were carried out with an anhydrous and hydrous sample under isothermal conditions. The anhydrous sample AndU0c was measured at a temperature of 1055 K; heating to this temperature required ~45 min. (Fig. 3a). After reaching the target temperature, the viscosity decreased dramatically to $10^{8.8}$ Pa · s. A subsequent experiment performed at the same run conditions using a rigid silica glass cylinder showed that thermal relaxation of the entire apparatus caused this decrease in viscosity and that ~35 min were required to achieve thermal equilibrium. It is emphasized that small changes in temperature of 5 to 10 K, as used during measurement cycles (Table 2), do not cause a significant effect due to thermal equilibration (see also Schulze et al., 1999). After thermal equilibration, the viscosity increased only slightly in the next 100 min but more strongly in the following period, approaching a value of 10^{12} Pa · s after ~500 min. A rough extrapolation from the range with small variation in viscosity (80 to 180 min) to the time when the target temperature was reached yields a viscosity of $10^{10.1}$ Pa · s (Fig. 3a). The evolution of viscosity as a function of time was similar in the isothermal run with the hydrous sample AndU1.9b at 860 K (Fig. 3b). After thermal equilibration, the viscosity only slightly increased during the time interval of 50 to 110 min. Extrapolation to the time when the target temperature of 860 K was reached (35 min) yields a value of $10^{9.5}$ Pa · s. Uncertainties of these extrapolations are estimated to be <0.3 log units.

After the viscosity measurements, the densities of anhydrous glasses were determined by the Archimedean method, with toluene as the immersion liquid (Table 3). The densities of the glasses after the high-pressure experiments cannot be compared directly with the density of the starting material because of compaction and relaxation processes under pressure. Ohlhorst et al. (2001) presented a linear relationship between the density and the water content for the Unzen andesite for glasses synthesized at 500 MPa. Extrapolating their data to a water content of 0.0 wt.% yields a density of 2661 ± 6 g/L at 500 MPa for the anhydrous glass. Compared with the starting material ($\rho_{0.1\ MPa}$ = 2636 ± 2 g/L), the densification of the material is only ~1%. The density of the anhydrous samples strongly increased after the viscosity experiments (by 2.6, 2.4, and 2.9%, respectively, for the samples AndU0a, AndU0b, and AndU0c, compared to the relaxed glass at 500 MPa). In addition, these samples became paramagnetic, which was simply detected using a hand magnet. In contrast to the anhydrous samples, the iron-bearing hydrous sample AndU1.9b was not paramagnetic after the viscosity experiment.

Back-scattered electron images of sample AndU0a collected with an electron microprobe after the run showed homogeneous glass on a scale down to 0.1 μm. This glass had the same composition as the starting material. Transmission electron microscopy images of samples AndU0a, AndU0c, and AndU1.9b, however, showed crystalline phases dispersed in a glassy groundmass (Fig. 4). The crystallites had a grain size of 10 to 50 nm and were distributed homogeneously throughout the sample. Crystals in the long-term run AndU0c were found to be larger than in the short-term run AndU0a. Unfortunately, the selected area diffraction patterns obtained on the samples did not allow an unambiguous identification of the crystalline phases because of the low precision of the d_{hkl} values. Because of the magnetic properties, it is likely that the crystalline phases in the anhydrous samples include magnetite. This is in agreement with observations from Regnard et al. (1981), who investigated the magnetic properties of magnetite crystals with similar grain sizes in oxidized obsidians. The absence of paramagnetism for the hydrous sample AndU1.9b may indicate

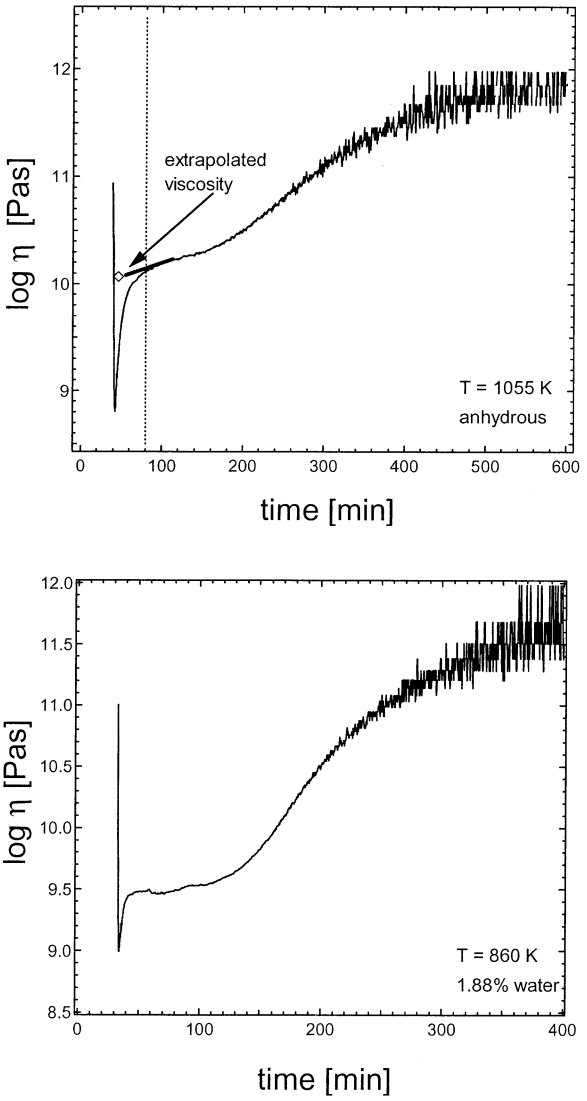

Fig. 3. (a) Viscosity vs. time during the run AndU0c (anhydrous melt) in an internally heated pressure vessel at 200 MPa. The dashed line represents the estimated time of thermal equilibration of the apparatus. The diamond symbol represents the extrapolated viscosity when the target temperature was reached. (b) Time evolution during the run AndU1.9b using a melt containing 1.88 wt.% H_2O. Note that the plots show only the initial stage of the runs and do not represent the whole run duration (see Table 3 for details).

Table 3. Overview of synthesis conditions, $Fe^{3+}/\Sigma Fe$ ratios, and densities of iron-bearing anhydrous and hydrous andesites investigated using high-pressure viscometry.

Sample	c^aH_2O	T (min)	T (K)	Extrapolated log η at T	$Fe^{3+}/\Sigma Fe$ initial	$Fe^{3+}/\Sigma Fe$ final	ρ_{final} (g/L)
AndU0a	0	170	998 to 1122	—	0.57	0.60	2730 (4)
AndU0b	0	750	1005 to 1086	—	0.57	0.57	2726 (2)
AndU0c	0	830	1055	10.1	0.57	0.55	2737 (6)
AndU1.9b	1.88 ± 0.05	600	860	9.5	0.33	0.35	n.a.[b]

The initial density of samples AndU0a-c is 2636 (±2) g/L at 0.1 MPa.
[a] Water content (wt%).
[b] Not analyzed.

the presence of a different iron oxide or hydroxide mineral instead of magnetite.

Complementary investigations were performed using NIR spectroscopy. Dramatic changes in the spectra were obtained after annealing. In contrast to the thermally untreated material, the viscosity samples were nearly opaque above 5000 cm^{-1} (Fig. 5). No significant differences in the spectra from various anhydrous samples with different run times were found. The high intensity of the NIR absorption features caused by the iron oxide phases did not allow changes in water content or iron redox state in the samples to be analyzed.

3.2. The Influence of Iron Redox State on Viscosity of Unzen Andesite

Viscosities of melts with different iron redox states were determined at ambient pressure. Synthesis conditions of samples, the FeO contents, and $Fe^{3+}/\Sigma Fe$ ratios before and after viscometry are given in Table 4. During the reduction of the melt, one end of the melt was in contact with the Ar/CO atmosphere, while the other end touched the graphite crucible. This resulted in a gradient of the $Fe^{3+}/\Sigma Fe$ ratio within the cylindrical samples. Presented $Fe^{3+}/\Sigma Fe$ ratios before viscometry are average values obtained from FeO analyses of glass pieces cut from the top (FeO_{top}) and the bottom (FeO_{bottom}) of the reduced glass cylinders. Differences in $Fe^{3+}/\Sigma Fe$ ratios calculated from FeO_{top} and FeO_{bottom} are included in Table 4. After viscosity measurements, glass cylinders were cracked, and a small piece was used for the final FeO determination. This final FeO value was used to evaluate the dependence of viscosity on $Fe^{3+}/\Sigma Fe$. However, microprobe analyses of the reduced glasses Unzen-2, Unzen-4, and Unzen-5 yielded slightly increased FeO_{total} values between 8.68 and 8.76 wt.% instead of 8.16 wt.% for the air-annealed starting material. These differences cannot be explained by loss of oxygen during the reduction and the subsequent calculation of total iron as FeO. We assume that systematic errors in the microprobe analyses, probably due to matrix effects or inhomogeneities in the reduced glasses, are responsible for these results. The essential point is that there is no evidence for iron loss to the capsule material. On the other hand, it is unlikely that addition of iron occurred during the synthesis of the reduced glasses. For comparison purposes, all $Fe^{3+}/\Sigma Fe$ ratios were calculated with 8.16 wt.% total iron given as FeO.

During the experiment with the oxidized material (Unzen-A) at ambient pressure, a time dependence of viscosity was first

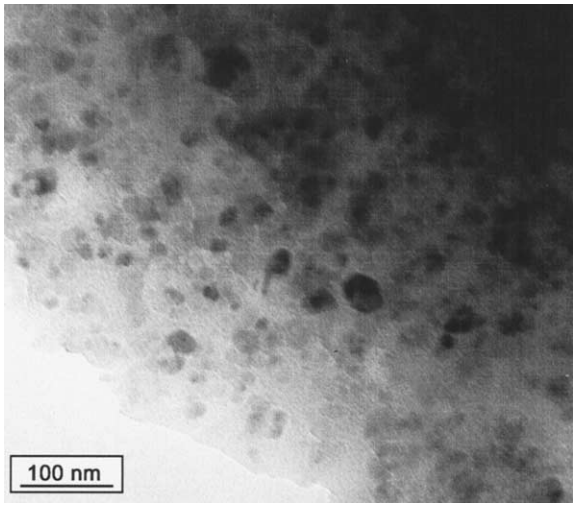

Fig. 4. Transmission electron microscopy picture of the edge of glass fragment after experiment AndU0c with a total run time of 830 min.

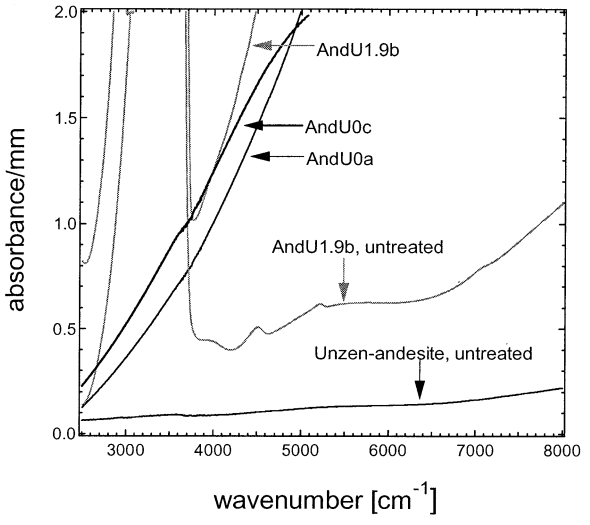

Fig. 5. Near-infrared absorption spectra of anhydrous (AndU0a, AndU0c: black lines) and hydrous (AndU1.9b: gray lines) iron-bearing samples before (untreated) and after viscometry. The bands at 4500 and 5200 cm^{-1} in the spectrum of the hydrous glass are due to combination modes of OH groups and H_2O molecules, respectively. The broad band near 3500 cm^{-1} is attributed to OH fundamental stretching vibrations.

Table 4. Sunthesis conditions and results from wet chemical FeO determination of iron-bearing anhydrous glasses.

Sample	Synthesis conditions	Atmosphere	FeO_{top} initial	FeO_{bottom} initial	$\Delta Fe^{3+}/\Sigma Fe$	$Fe^{3+}/\Sigma Fe$ initial	FeO final	$Fe^{3+}/\Sigma Fe$ final
Unzen-A	1873 K	Air	3.53		—	0.57	3.40	0.58
Unzen-3	1573 K, 20 min	Ar/CO	4.41	5.40	0.11	0.40	4.90	0.40
Unzen-2	1573 K, 40 min	Ar/CO	5.68	6.75	0.12	0.24	5.40	0.34
Unzen-4	1573 K, 120 min	Ar/CO	6.00	6.55	0.06	0.23	6.43	0.21
Unzen-5	1573 K, 180 min	Ar/CO	6.83	7.23	0.05	0.14	6.44	0.21

Melts reduced in an Ar/CO atmosphere were stored in a graphite crucible.
$\Delta Fe^{3+}/\Sigma Fe$ denotes the difference between $Fe^{3+}/\Sigma Fe$ ratios calculated from FeO_{top} and FeO_{bottom}.

observed after 120 min at a temperature of 1108 K. Heating and thermal equilibration of the apparatus in this experiment required 30 min, and the data acquisition for each viscosity measurement took between 1 and 10 min, depending on the temperature. Reliable viscosity data could be obtained before the onset of noticeable crystallization because every viscosity at a given temperature was checked for time dependence. During the run with the partially reduced sample Unzen-3, a time dependence of viscosity was observed after 100 min (after temperature step 4; see Table 5), and the sample became paramagnetic. The consistency to the viscosity data obtained at steps 1 and 3 implies that the measurement at step 4 was not yet influenced noticeably by crystallization. In contrast, the most reduced samples (Unzen-2, Unzen-4, and Unzen-5; run times of 150, 120, and 130 min, respectively) showed no time dependence with regard to viscosity. This suggests that crystallization of iron-bearing phases is strongly related to the abundance of ferric iron.

The viscosity of the reduced sample Unzen-5 is, on average, 1.7 log units lower than that of the sample Unzen-A, which was synthesized in air (Fig. 6, Table 5). This corresponds to a difference in temperature of 57 K. Compared with the iron-free analog, the difference is 2.4 log units and 80 K, respectively. Viscosities of the samples Unzen-2, Unzen-4, and Unzen-5 are identical within experimental error. As shown in Figure 7a, the viscosity changes nonlinearly with the $Fe^{3+}/\Sigma Fe$ ratio, with the largest variation at high $Fe^{3+}/\Sigma Fe$ ratio. On the other hand, the data for activation energy of viscous flow show no clear evidence for a nonlinear relationship to $Fe^{3+}/\Sigma Fe$ (Fig. 7b).

4. DISCUSSION

4.1. The Effect of Pressure on the Viscosity

In the literature, the degree of melt depolymerization quantified as NBO/T (nonbridging oxygen per tetrahedron) is used as a parameter determining the dependence of viscosity on pressure (Brearley et al., 1986; Scarfe et al., 1987; Bottinga and Richet, 1995). Scarfe et al. (1987) found an isothermal decrease in viscosity with increasing pressure (negative pressure effect) for melts with NBO/T $<$ 1 and an isothermal increase in viscosity with increasing pressure (positive pressure effect) for melts with NBO/T $>$ 1 on the basis of data obtained from falling sphere experiments on different synthetic and natural melts. However, it is difficult to compare these data with our results because the falling sphere data were obtained at superliquidus temperatures. To our knowledge, the only experimental viscosity data with regard to pressure effects in the glass transition range were reported by Schulze et al. (1999) and Schulze (2000). In the system albite-diopside (Ab-Di), Schulze (2000) observed a positive pressure effect at an NBO/T of 0.32 (composition $Ab_{74}Di_{26}$) (Fig. 8). Their data indicate a crossover between a positive and negative dependence on viscosity between an NBO/T of 0.1 to 0.3, depending on the melt viscosity.

The pressure dependence of viscosity, expressed as $d\log\eta/dP$, was calculated for the model andesite from the slopes of linear regressions (Figs. 2a to 2c) at a temperature at which the model of Richet et al. (1996) predicts a viscosity of 10^{10} Pa · s. The NBO/T ratio was calculated from Persikov (1991), assuming that all the water is dissolved in the form of hydroxyl groups and thus acts as a network modifier. It is emphasized that the dissolution of water in aluminosilicate melts and glasses may be more complex than expressed in this simple model and that the presence of hydroxyl groups does not necessarily require depolymerization (see review of Kohn, 2000). Nevertheless, the NBO/T concept is a useful approximation for hydrous melts, at least at low water concentrations, to quantify the pressure dependence on the viscosity.

The viscosity of the anhydrous iron-free andesite in this

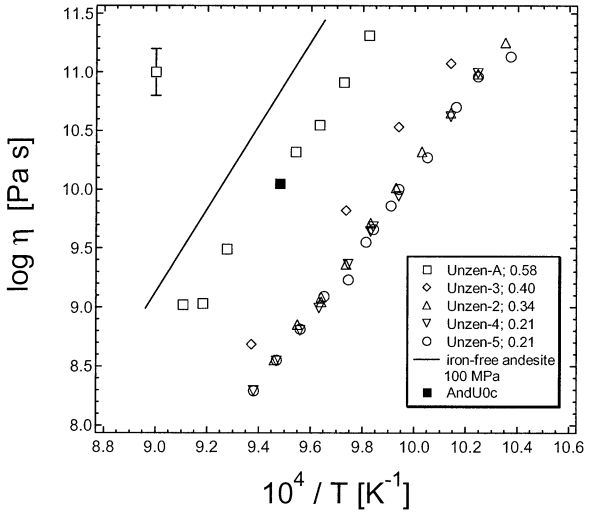

Fig. 6. Results from viscosity measurements of iron bearing andesites at ambient pressure with the thermomechanical analysis dilatometer. Values behind sample numbers refer to $Fe^{3+}/\Sigma Fe$ ratios. The solid line represents the Arrhenian fit of the iron-free andesite at 100 MPa pressure. The solid square represents the extrapolated data point from run AndU0c at 200 MPa (see Fig. 3a)

Table 5. Viscosity data and fit parameter of iron-bearing andesitic melts with different oxidation states measured at atmospheric pressure.

Unzen-A			Unzen-3			Unzen-2			Unzen-4			Unzen-5		
T (K)	log η	No.	T (K)	log η	No.	T (K)	log η	No.	T (K)	log η	No.	T (K)	log η	No.
1018	11.31	3	986	11.07	3	966	11.25	2	976	10.99	4	964	11.13	9
1028	10.91	4	1006	10.53	2	976	10.98	8	986	10.62	3	976	10.96	4
1038	10.55	2	1027	9.82	4	986	10.65	3	1006	9.94	2	984	10.70	10
1048	10.32	5	1067	8.68	1	997	10.32	4	1016	9.68	10	995	10.27	2
1078	9.49	6				1007	10.01	9	1017	9.64	5	1006	10.00	5
1089	9.03	1				1017	9.71	10	1026	9.36	6	1009	9.86	13
1098	9.02	7				1027	9.36	5	1038	8.99	1	1016	9.66	3
						1037	9.04	1	1046	8.80	7	1019	9.55	8
						1037	9.08	6	1056	8.54	8	1026	9.23	1
						1047	8.85	11	1066	8.29	9	1036	9.09	6
						1057	8.55	7				1046	8.81	11
												1056	8.55	7
												1066	8.29	12
A		–20.70 (1.22)		–20.75 (0.85)			–20.69 (0.35)			–20.99 (0.41)			–19.91 (0.66)	
$B \times 10^{-4}$		3.26 (0.13)		3.14 (0.09)			3.09 (0.04)			3.12 (0.04)			3.00 (0.07)	
E_a		622 (25)		601 (17)			592 (7)			597 (8)			575 (12)	

No. refers to the sequence of measurement.

study (NBO/T = 0.23) is nearly independent of pressure in the investigated temperature range. Hydrous samples show a positive pressure effect on the viscosity, probably resulting from an increased depolymerization of the melts. The errors in the $d\log\eta/dP$ values are relatively large for the iron-free andesite because the data are based on two different experimental data sets obtained from melts with slightly different chemical compositions. In addition, the regressions are based only on three to four data points, which is insufficient for a rigorous statistic treatment. Nevertheless, the data are in good agreement with the trend observed by Schulze (2000) for the chemically different albite-diopside system, which implies that NBO/T may be a suitable parameter to estimate the pressure dependence of viscosity for other silicate compositions. As shown in Figure 8, the variation of $d\log\eta/dP$ with NBO/T is especially large for highly polymerized melts (NBO/T $<$ 0.5) but small for depolymerized melts. However, the data in Figure 8 do not correspond to the same temperature but to the same melt viscosity at a reference temperature and pressure. Data for the Ab-Di join were calculated at a temperature corresponding to 10^{10} Pa · s at 200 MPa. Reference temperatures for andesite melts refer to 10^{10} Pa · s at ambient pressure calculated with the model of Richet et al. (1996) (for temperature values, see Figs. 2a to 2c).

4.2. The Influence of Iron on the Viscosity

Neuville et al. (1993) explained the observed continuous increase of the viscosity of andesitic melts with time by a progressive oxidation of ferrous to ferric iron and subsequent crystallization of magnetite. Figure 9 compares the $Fe^{3+}/\Sigma Fe$ values of all viscosity samples used in our study before and after measurements. In the high-pressure experiment, the redox state of both the anhydrous and the hydrous samples did not noticeably change. At ambient pressure, two of the samples with low initial $Fe^{3+}/\Sigma Fe$ apparently became more oxidized during the run (Unzen 2 and Unzen 5). However, $<$ 10 wt.% of each viscosity sample was used for the final FeO determination, so the analysis may not be representative for the whole sample.

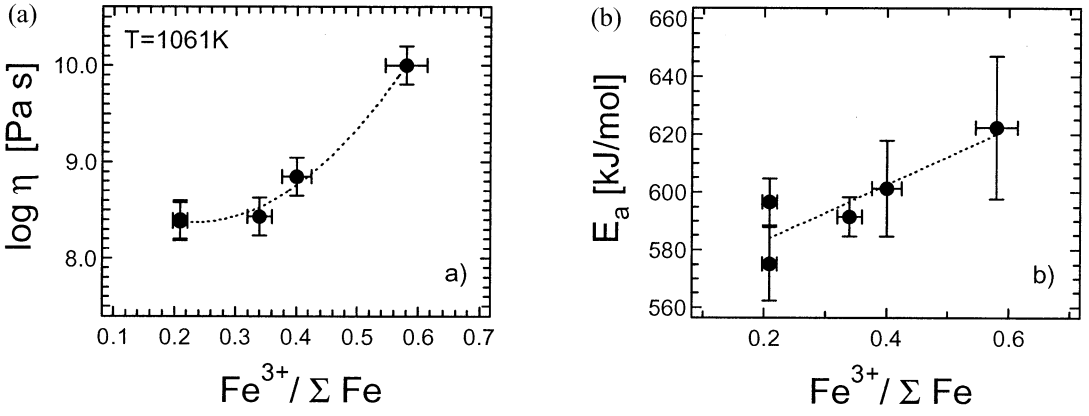

Fig. 7. (a) Viscosity and (b) activation energy of the viscous flow of iron-bearing andesites at ambient pressure as a function of $Fe^{3+}/\Sigma Fe$.

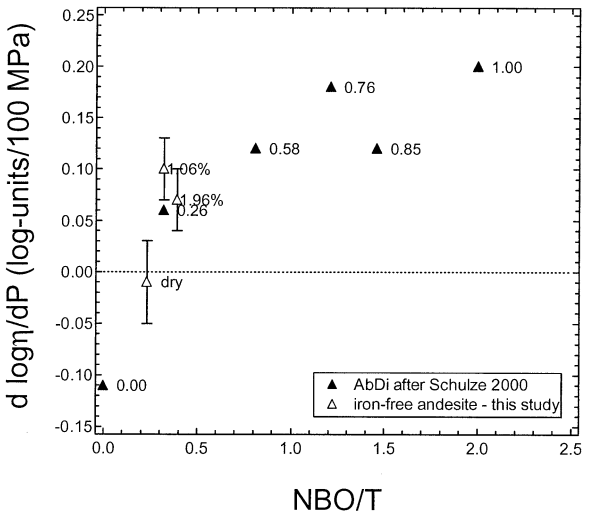

Fig. 8. Pressure dependence of the viscosity ($d\log\eta/dP$) as a function of depolymerization of the melt at a constant viscosity of 10^{10} Pa · s. Values behind data points from Schulze (2000) refer to the mole fraction of the diopside component. The water concentration in the andesitic melts is shown next to the corresponding data points. The error bars for the iron-free andesite represent only the standard deviation from the linear regression. For further explanations, see text. NBO/T = nonbridging oxygen per tetrahedron.

On the other hand, even if there was a progressive superficial oxidation of iron, this had no significant influence on the physical properties of the entire specimen. For samples Unzen 2 and Unzen 5, viscosities determined at similar temperatures but at different times during the measurement cycle are consistent.

Richet et al. (1996) stated as well that the $Fe^{3+}/\Sigma Fe$ ratio of their air-annealed andesitic sample was nearly identical before and after the viscometry. They suggested that the change of composition of the residual melt due to the partial crystallization had caused the increase in viscosity. However, both network-forming Fe^{3+} and network-modifying Fe^{2+} are extracted by crystallization of magnetite so that the change in calculated NBO/T is only minor. Assuming complete extraction of magnetite from our oxidized melt ($Fe^{3+}/\Sigma Fe$ = 0.57, 5.15 wt.% Fe_2O_3 and 3.23 wt.% FeO), the residual amount of dissolved FeO is 1.3 wt.%, and the calculated NBO/T of the melt changes from 0.23 to 0.24. Such a small increase in NBO/T would have a negligible influence on the viscosity of the melt and would rather result in a decrease in viscosity. Hence, this is not in agreement with the experimental results.

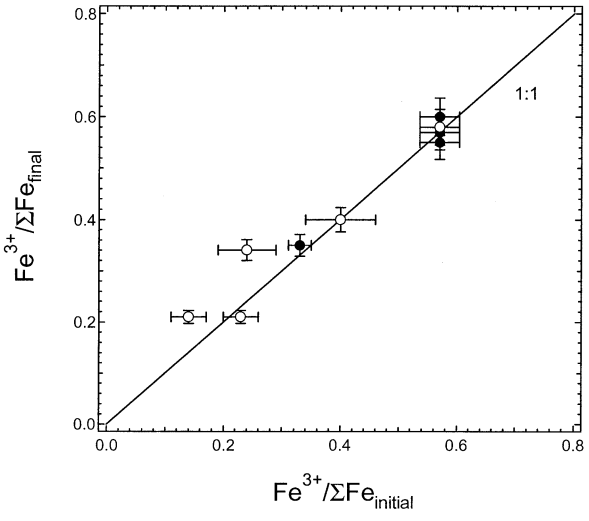

Fig. 9. $Fe^{3+}/\Sigma Fe$ ratios before and after viscometry of all samples used in this study. Filled symbols refer to high-pressure experiments, open symbols to measurements at ambient pressure.

Another possible explanation for the increase in viscosity is strengthening of the sample due to the crystal fraction. Lejeune and Richet (1995) performed an experimental study of viscosities as a function of the crystal content in the system $Mg_3Al_2Si_3O_{12}$. They found that a fraction of < 40 vol.% of spherical crystals has a relatively small effect on the viscosity. Assuming complete extraction of iron from the andesite melt as magnetite, the maximum weight proportion of magnetite can be only 7.45%. This would result in a lower volume fraction due to the higher specific density of magnetite compared to silicate melts. Both magnetite and garnet (crystallized in the study of Lejeune and Richet, 1995) are cubic minerals, so that the effect on rheological properties of magmas is expected to be similar, in contrast, for instance, to needle-like minerals such as amphiboles or pyroxene, for which the increase of viscosity per volume percentage of crystal is expected to be larger (e.g., Stevenson et al., 2001). Furthermore, Lejeune and Richet (1995) found no significant change in viscosity as a function of time for a rapidly crystallizing $Li_2Si_2O_5$ sample with crystal fractions up to 19 vol.%. Hence, the presence of crystals and their growth cannot alone explain the observed viscosity-time behavior during our measurements. However, the crystal diameter of ~180 to 400 μm was much larger in the study of Lejeune and Richet (1995) than in our study, and therefore, the mean distance between the crystals also was much larger, so that their results may be not directly transferable. Assuming an average crystal diameter of 20 nm and complete crystallization of iron as magnetite, the average distance between the crystals is only ~50 nm. Across this short distance, there might be an interaction of the minerals. Also, the structure of the melt in between the crystals might be different from that of the bulk melt. On the other hand, a time dependence in melt viscosity of the andesite samples is observed rapidly after reaching the glass transition temperature. This implies that even the initial stage of crystallization, which involves clustering of iron atoms to form crystal nuclei and transport of iron to the growing crystals, strongly affects the melt structure. This interpretation is supported by a recent study of Wilke et al. (2002), who observed differences in X-ray absorption spectra from iron-bearing glasses cooled down with different quench rates. Spectra of slowly quenched glasses show evidence for a highly ordered medium-range environment around Fe. The formation of iron clusters might be a reason for the initial increase of melt viscosity observed for the oxidized andesite samples. A detailed explanation, however, cannot be given on the basis of our present knowledge.

In conclusion, whether or not viscosity data representative for the uncrystallized, iron-rich melt can be obtained depends mainly on the time required for thermal equilibration of the

apparatus and for data acquisition. Using the dilatometric method, viscosities of anhydrous andesite melts could be measured in the range 10^8 to 10^{11} Pa · s for ~70 to 90 min after a period of 25 to 30 min of heating and thermal equilibration. However, the time until crystallization perturbs the viscosity measurement may depend strongly on temperature. Crystallization may occur directly after thermal equilibration at initial viscosities $< 10^9$ Pa · s because of fast diffusion in the melt. Using the high-pressure apparatus of Schulze et al. (1999), the viscosity can be determined only at a single temperature by extrapolating the viscosity to the time when the run temperature was reached. It is noteworthy that this extrapolation at 1055 K and 200 MPa yields a viscosity that is in excellent agreement with the 1 atm data measured using the dilatometer (Fig. 6).

4.3. The Influence of Iron Redox Condition on the Viscosity

Using NBO/T as the parameter to describe the compositional dependence of viscosity, the effect of iron redox state on the viscosity of andesitic melts (Fig. 6) can be rationalized as the transformation of a network former (Fe^{3+}) into a network modifier (Fe^{2+}). However, a direct correlation between viscosity and degree of depolymerization is difficult because of the complexity of iron incorporation in silicate glasses and melts and because of the lack of structural information for andesitic melts. Under oxidizing conditions, ferric iron is predominantly in tetrahedral coordination in silicate glasses (e.g., Virgo and Mysen, 1985). On the basis of isomeric shifts obtained from Mössbauer data, Mysen (1991) concluded that an octahedral coordination is preferred by ferric iron under reducing conditions. A change of coordination from tetrahedral to octahedral in the system Na_2O-Al_2O_3-SiO_2-Fe-O is completed at $Fe^{3+}/\Sigma Fe < 0.3$. The coordination of ferrous iron in silicate glasses is controversial in the literature. Virgo and Mysen (1985), Fox et al. (1981), and Wang et al. (1995) favored ferrous iron being in octahedral coordination, whereas Waychunes et al. (1988) and Brown et al. (1995) found evidence for tetrahedrally and fivefold coordinated Fe^{2+} from spectroscopic data. Recently, Galoisy et al. (2001) presented high-resolution X-ray absorption near-edge structure spectra from volcanic glasses and found that ferrous iron is mostly in fivefold coordination and in minority fourfold coordinated, whereas ferric iron occurs in both in fourfold and sixfold coordinated sites.

Because of the complexity of the structural role of iron in silicate melts, the concept of NBO/T is only a crude approach to predicting the compositional variation of melt viscosity. The limits of this approach are obvious when comparing viscosity data of the natural andesite and its iron-free analog. Assuming all Fe^{2+} to be network modifier and all Fe^{3+} to be network former, both melt compositions have the same NBO/T of 0.23 after synthesis in air ($T = 1873$ K, $\log_{10} fO_2 = -0.67$). The viscosities, however, differ by 0.7 log units (Fig. 6) on average at temperatures between 1018 and 1136 K. This may be explained by differences in bond strength and coordination of Fe^{2+} and Fe^{3+} compared to their substitutes Mg^{2+}, Ca^{2+}, and Al^{3+}, respectively, probably because of the contributions of the d-electrons in interatomic bonds. However, even when the viscosities of iron-free melts with similar degree of depolymerization are compared, it is evident that the concept of NBO/T is only a raw approach to quantifying compositional trends. For example, the temperature at which the melt viscosity equals 10^{12} Pa · s is 100 K lower for a synthetic phonolitic melt (NBO/T = 0.19, $T_{12} = 919$ K; Whittington et al., 2001) than for our iron-free andesitic melt (NBO/T = 0.23, $T_{12} = 1019$ K). The nonlinear variation of viscosity with $Fe^{3+}/\Sigma Fe$ (Fig. 6a) also indicates a complex structural role for iron in andesitic melts. The same general behavior was observed for other iron-bearing silicate melts. Cukierman and Uhlmann (1974) reported a dramatic decrease in viscosity by 3 orders of magnitude for a lunar composition in the high-viscosity range when changing the $Fe^{3+}/\Sigma Fe$ ratio from 0.80 to 0.24. Further reduction of $Fe^{3+}/\Sigma Fe$ had a negligible effect on viscosity. In the system Na_2O-FeO-Fe_2O_3-SiO_2 at superliqudius conditions, Dingwell and Virgo (1987) found the change of melt viscosity with $Fe^{3+}/\Sigma Fe$ to be most pronounced for $Fe^{3+}/\Sigma Fe > 0.5$. However, the overall effect of iron redox state on the viscosity appears to be much smaller in the low- vs. high-viscosity range. Dingwell and Virgo (1987) found a decrease in viscosity of 0.81 log units at 1473 K when the $Fe^{3+}/\Sigma Fe$ ratio of their NS4F40 (0.6 $Na_2Si_4O_9$ + 0.4 · $Na_6Fe^{3+}{}_4O_9$) melt changed from 1.00 to 0.28. A decrease in viscosity by 0.34 log units was observed for a $NaFeSi_2O_6$ (acmite) melt when decreasing the $Fe^{3+}/\Sigma Fe$ ratio from 0.92 to 0.18 at 1703 K. In our study, the difference in viscosity between the oxidized sample Unzen-A ($Fe^{3+}/\Sigma Fe = 0.58$) and the reduced sample Unzen-5 ($Fe^{3+}/\Sigma Fe = 0.21$) was found to be 1.6 log units at 1061 K.

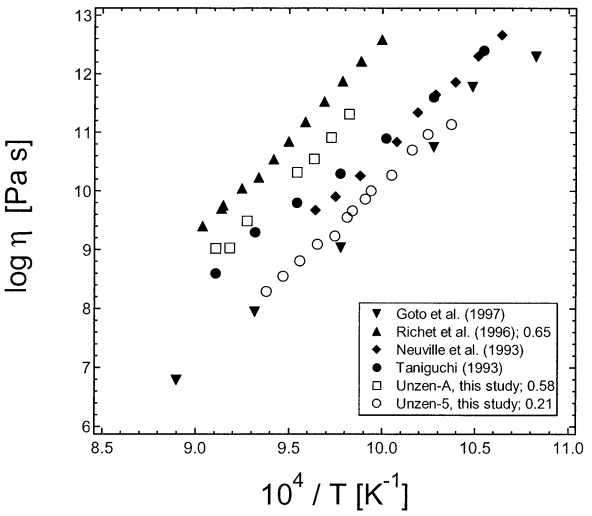

Fig. 10. Comparison of viscosity data for iron-bearing andesites measured at ambient pressure. Data next to references refer to the $Fe^{3+}/\Sigma Fe$ ratio of the melt.

4.4. Comparison With Literature Data of Iron-Bearing Andesites

In Figure 10, viscosity data for andesitic melts at ambient pressure from our study are compared to previous studies. Viscosities were obtained either by parallel-plate viscometry (Neuville et al., 1993; Richet et al., 1996) or by fiber elongation (Taniguchi, 1993; Goto et al., 1997). SiO_2 concentrations of the melts ranged from 56.65 to 61.17 wt.%. The samples in all these studies were melted and equilibrated in air. At a given

temperature, the data cover a viscosity range of ~2 orders of magnitude. These differences may partly be explained by different chemical compositions used in these studies. Alternative explanations for this result include (1) different redox states of iron in the samples and/or (2) different experimental procedures:

1. Information about iron redox state in the samples used for viscosity measurement are given only by Richet et al. (1996). The $Fe^{3+}/\Sigma Fe$ ratio of 0.65 of their andesite from Mt. Pelée is slightly higher than in our air-annealed samples (0.58). Their results are consistent with the evolution of viscosity with $Fe^{3+}/\Sigma Fe$ observed in our study.
2. As shown above, pretreatment of the samples and the heating procedure during the viscosity experiment may have a strong effect on the viscosity data because of the onset of crystallization. Taniguchi (1993) annealed the samples for 30 min at the glass transition temperature T_g (roughly measured by the dilatometric method) plus 15 K (Taniguchi and Murase, 1987) to eliminate thermal strain, whereas Goto et al. (1997) used untreated samples to prevent redox changes of iron. During the measurements of Neuville et al. (1993) and Richet et al. (1996), their creep apparatus required ~15 to 20 min at 1073 K for thermal equilibration (Neuville, 1992). The general trend in the time evolution of viscosity observed by Neuville et al. (1993) and Richet et al. (1996) is similar to the run AndU0c (Fig. 3a), but the time scale is different. Neuville et al. (1993) found an increase in viscosity of ~1 log unit from an initial value of $10^{10.7}$ Pa · s within 1200 min, whereas Richet et al. (1996) reported a similar increase at an initial viscosity of $10^{10.2}$ Pa · s after annealing for 6000 min. This contrasts with our observation, in which an increase in viscosity of > 1.5 log units (starting at $10^{10.1}$ Pa · s) occurred in < 500 min after thermal equilibration of the apparatus (Fig. 3a). However, Neuville et al. (1993) and Richet et al. (1996) applied stresses of up to 50 MPa to their samples, whereas in our study, the maximum stress was much lower (~0.9 MPa in the high-pressure viscometer and ~0.3 MPa in the dilatometer). This may indicate that the time evolution of viscosity is dependent on the applied stress. In conclusion, because of the use of different experimental apparatus and procedures, it is not possible to decide whether or not the viscosities derived in the previous studies are affected by crystallization.

4.5. Application of Data From Model Compositions to Natural Systems

Application of empirical models of melt viscosities to natural systems may be difficult because many parameters (temperature, pressure, bulk composition, H_2O content, oxygen fugacity) must be taken into account and are often poorly constrained. The empirical model of Richet et al. (1996) is based on experimental viscosity data of andesitic melts over a temperature interval from 996 to 1978 K and water concentrations up to 3.5 wt.% H_2O. However, it does not consider the effects of pressure and oxygen fugacity. Although the influence of pressure on viscosity may be small when compared with temperature and water content, it is nevertheless important for geological applications to know if there is an increase or a decrease of the viscosity with pressure. For example, crystal fractionation will be more effective with depth if the viscosity decreases with increasing pressure.

More important is the effect of the iron redox state on the viscosity of natural melts. Investigations by Fudali (1965) showed that andesites often equilibrate with an oxygen fugacity close to the Ni-NiO (NNO) buffer. Under these redox conditions, the $Fe^{3+}/\Sigma Fe$ ratio is relatively low (<0.5). The average $Fe^{3+}/\Sigma Fe$ of andesites ranges between 0.36 (Nockolds, 1954) and 0.41 (Chayes, 1975). Richet et al. (1996) reported very good agreement in the viscosity between their iron-free andesite and a natural sample from Mt. Pelée measured from 1000 to 1107 K. The natural andesite was reequilibrated in air before viscometry and yielded a $Fe^{3+}/\Sigma Fe$ ratio of 0.65. Thus, it was much more oxidized than a melt equilibrated under the estimated magma storage conditions of ~NNO + 0.4 to NNO + 0.8 (Martel et al., 1998) for the Mt. Pelée andesite. As a consequence, application of Richet et al's (1996) model may significantly overestimate the viscosity of anhydrous andesitic melts at temperatures near the glass transition. For example, at 1057 K, the calculated viscosity of $10^{10.67}$ Pa · s is 2.12 log units higher than the measured value for the sample Unzen-2 with $Fe^{3+}/\Sigma Fe = 0.34$ (Table 5). However, it is difficult to verify the model of Richet et al. (1996) for hydrous melts because of the lack of experimental data. The estimated viscosity of $\sim 10^{9.5}$ Pa · s at 860 K for an andesitic melt containing 1.88 wt.% H_2O (run AndU1.9b, Fig. 3b) is only 0.7 log units lower than predicted by Richet et al. (1996). In this experiment, the intrinsic oxygen fugacity of the IHPV (~NNO + 2) was more similar to natural conditions. This result indicates that the empirical model of Richet et al. (1996) may be more suitable for hydrous melts than for dry melts. Furthermore, the differences in viscosity between oxidized and reduced melts appear to be smaller in the low-viscosity range than in the high-viscosity range. Thus, the model of Richet et al. (1996) can yield a reasonable first estimate of the viscosity of hydrous andesitic melts at magmatic conditions.

5. CONCLUSIONS

The dominant parameters controlling the viscosity of andesite melts are the temperature and the water content. The results of Richet et al. (1996) show that the viscosity of an iron-free andesite melt decreases by 12 orders of magnitude when the temperature increases from 996 to 1978 K. Adding 3.46 wt.% H_2O to the melt at 1000 K decreases the viscosity by 7 orders of magnitude. The results from our study indicate that the influence of pressure on the viscosity is much smaller. The pressure effect is negligible for anhydrous andesitic melt. In melts containing between 1 and 2 wt.% H_2O, increasing pressure from 0.1 to 300 MPa increases the viscosity by up to half an order of magnitude. The observed pressure effects are consistent with results of Schulze (2000) for melts along the join Ab-Di, indicating a positive correlation between the degree of melt polymerization and the pressure dependence for viscosity.

Investigation of iron-bearing andesites in the high-viscosity range is complicated by structural changes in the melts during nucleation and growth of iron oxide minerals. These processes are strongly related to the presence of ferric iron. Our results indicate that viscosity data representative for the homogenous

(uncrystallized) melt can be obtained only within 100 to 120 min at temperatures near the glass transition.

A change in iron redox state has a large effect on the viscosity of andesitic melts, particularly under oxidizing conditions. At 1061 K, a decrease in $Fe^{3+}/\Sigma Fe$ from 0.58 to 0.40 causes a viscosity decrease of 1.1 log units. Further decrease of $Fe^{3+}/\Sigma Fe$ to 0.21 reduces the viscosity by only 0.5 log units.

The application of melt viscosity data obtained on melts equilibrated in air leads to an overestimate in the viscosity of natural melts by up to 2 orders of magnitude, depending on the water content. The empirical model of Richet et al. (1996) is suitable for calculating the effect of water and temperature on the rheology of andesitic melts. However, because of the substitution of iron by Mg and Ca in the andesite analog composition used in their viscosity study, the model tends to overestimate the viscosity of natural systems with an oxygen fugacity close to the NNO buffer.

Acknowledgments—This study was supported by the DAAD/NSF cooperation program and by the German Science Foundation (project Be1720/12). We thank Otto Dietrich, Willy Hurkuck, and Bettina Aichinger for technical support. We would like to thank Claudia Romano for editorial handling of this paper and Alan Whittington and two anonymous reviewers for their helpful comments.

Associate editor: C. Romano

REFERENCES

Behrens H., Romano C., Nowak M., Holtz F., and Dingwell D. B. (1996) Near-infrared spectroscopic determination in glasses of the system $MAlSi_3O_8$ (M=Li, Na, K): An interlaboratory study. *Chem. Geol.* **128,** 41–63.

Berndt J., Liebske C., Holtz F., Freise M., Nowak M., Ziegenbein D., Hurkuck W., and Koepke J. (2002) A combined rapid-quench and H_2-membrane setup for internally heated pressure vessels: Description and application for water solubility in basaltic melts. *Am. Mineral.* **87,** 1717–1726.

Bottinga Y. and Richet P. (1995) Silicate melts: The "anomalous"pressure dependence of the viscosity. *Geochim. Cosmochim. Acta* **59,** 2725–2731.

Brearley M., Dickinson J. E. Jr., and Scarfe C. M. (1986) Pressure dependence of melt viscosities on the join diopside-albite. *Geochim. Cosmochim. Acta* **50,** 2563–2570.

Brown G. E. J., Farges F., and Calas G. (1995) X-ray scattering and X-ray spectroscopy studies of silicate melt. *Rev. Mineral.* **32,** 317–410.

Chayes F. (1975) A world data base for igneous petrology. *Carneg. Inst. Wash. Year Book* **74,** 549–550.

Chen H. C., DePaolo D. J., Nakada S., and Shieh Y. M. (1993) Relationship between eruption volume and neodymic isotopic composition at Unzen vulcano. *Nature* **362,** 831–834.

Cukierman M. and Uhlmann D. R. (1974) Effects of iron oxidation state on viscosity, Lunar composition 15555. *J. Geophys. Res.* **79,** 1594–1598.

Dingwell D. B. (1986) Viscosity-temperature relationships in the system $Na_2Si_2O_5$-$Na_4Al_2O_5$. *Geochim. Cosmochim. Acta* **50,** 1261–1265.

Dingwell D. B. (1989) Shear viscosities of ferrosilicate liquids. *Am. Mineral.* **74,** 1038–1044.

Dingwell D. B. (1991) Redox viscometry of some Fe-bearing silicate melts. *Am. Mineral.* **76,** 1560–1562.

Dingwell D. B. and Mysen B. O. (1985) Effects of water and fluorine on the viscosity of albite melt at high pressure; a preliminary investigation. *Earth Planet. Sci. Lett.* **74,** 266–271.

Dingwell D. B. and Virgo D. (1987) The effect of oxidation state on the viscosity of melts in the system Na_2O-FeO-Fe_2O_3-SiO_2. *Geochim. Cosmochim. Acta* **51,** 195–205.

Dingwell D. B., Romano C., and Hess K. U. (1996) The effect of water on the viscosity of a haplogranitic melt under P-T-X conditions relevant to silicic volcanism. *Contrib. Mineral. Petrol.* **124,** 19–28.

Fox K. E., Furukava T., and White W. B. (1981) Transition metal ions in silicate melts. Part 2. Iron in sodium silicate glasses. *Phys. Chem. Glasses* **23,** 169–178.

Fudali R. F. (1965) Oxygen fugacities of basaltic and andesitic magmas. *Geochim. Cosmochim. Acta* **29,** 1063–1075.

Galoisy L., Calas G., and Arrio M. A. (2001) High resolution XANES spectra of iron in minerals and glasses: Structural information from the pre-edge region. *Chem. Geol.* **174,** 307–319.

Goto A., Maeda I., Nishida Y., and Oshima H. (1997) Viscosity—Equation for magmatic silicate melts over a wide temperature range. In *Proceedings Unzen Intern; Workshop: Decade Vulcano and Scientific Drilling*, pp. 100–105. Shimabara, Japan.

Kilinc A., Carmichael I. S. E., Rivers M. L., and Sack R. O. (1983) The ferric-ferrous ratio of natural silicate liquids equilibrated in air. *Contrib. Mineral. Petrol.* **83,** 136–140.

Klein L. C., Fasano B. V., and Wu J. M. (1983) Viscous flow behavior of four iron-containing silicates with alumina, effects of composition and oxidation condition. *J. Geophys. Res., Suppl.* **88,** A880–A886.

Kohn S. C. (2000) The dissolution mechanims of water in silicate melts; a synthesis of recent data. *Mineral. Mag.* **64,** 389–408.

Kushiro I., Yoder J. R., and Mysen B. O. (1976) Viscosities of basalt an andesite melts at high pressures. *J. Geophys. Res.* **81,** 6351–6356.

Lange R. A. and Carmichael I. S. E. (1989) Ferric-ferrous equilibria in NaO-FeO-FeO-SiO melts: Effects of analytical techniques on derived partial molar volumes. *Geochim. Cosmochim. Acta* **53,** 2195–2204.

Lejeune A. M. and Richet P. (1995) Rheology of crystal-bearing silicate melts: An experimental study at high viscosities. *J. Geophys. Res.* **100,** 4215–4229.

Martel C., Pichavant M., Bourdier J. L., Traineau H., Holtz F., and Scaillet B. (1998) Magma storage conditions and control of eruption regime in silicic volcanoes: Experimental evidence from Mt. Pelee. *Earth Planet. Sci. Lett.* **156,** 89–99.

Montenero A., Friggeri M., Giori D. C., Belkhiria N., and Pye L. D. (1986) Iron-soda-silica glasses: Preparation, properties, structure. *J. Non-Cryst. Solids* **84,** 45–60.

Mysen B. O. (1991) Relation between structure, redox equlibria of iron, and properties of magmatic liquids. *Adv. Phys. Chem.* **9,** 41–98.

Mysen B. O., Virgo D., Scarfe C. M., and Cronin D. J. (1985) Viscosity and structure of iron- and aluminum-bearing calcium silicate melts at 1 atm. *Am. Mineral.* **70,** 487–498.

Neuville D. R. (1992) *Etude des Propriétes Thermodynamiques et Rhéologiques des Silicates Fondus*. Ph.D. thesis, Universite Paris 7.

Neuville D. R. and Richet P. (1991) Viscosity and mixing in molten (Ca, Mg) pyroxenes and garnets. *Geochim. Cosmochim. Acta* **55,** 1011–1019.

Neuville D. R., Courtial C., Dingwell D. B., and Richet P. (1993) Thermodynamic and rheological properties of rhyolite and andesite melts. *Contrib. Mineral. Petrol.* **113,** 572–581.

Nockolds S. R. (1954) Average chemical composition of some igneous rocks. *Bull. Geol. Sc. Am.* **65,** 1007–1032.

Ohlhorst S., Behrens H., and Holtz F. (2001) Compositional dependence of molecular absorptivities of near-infrared OH- and H_2O bands in rhyolitic to basaltic glasses. *Chem. Geol.* **174,** 5–20.

Persikov E. S. (1991) The viscosity of magmatic liquids: Experiment, generalized patterns. A model for calculation and prediction. *Appl. Adv. Phys. Chem.* **9,** 1–41.

Regnard J. R., Chavez-Rivas F., and Chappert J. (1981) Study of the oxidation states and magnetic properties of iron in volcanic glasses: Lipari and Teotohuacan obsidians. *Bull. Mineral.* **104,** 204–210.

Richet P., Lejeune A. M., Holtz F., and Roux J. (1996) Water and the viscosity of andesite melts. *Chem. Geol.* **128,** 185–197.

Scarfe C. M., Cronin D. J., Wenzel J. T., and Kauffman D. A. (1983) Viscosity-temperature relationships at 1 atm in the system diopside-anorthite. *Am. Mineral.* **68,** 1083–1088.

Scarfe C. M., Mysen B. O., and Virgo D. (1987) Pressure dependence of the viscosity of silicate melts. In *Magmatic Processes: Physicochemical Principles, Vol. Special Publication No. 1* (ed. B. O. Mysen), pp. 504–511. The Geochemical Society, St. Louis, MO.

Schulze F. (2000) *Untersuchung zum Einfluβ von Druck und gelöstem Wasser auf die Viskosität silikatischer Schmelzen—Anwendung eines "parallel-plate"-Viskosimeters unter hohen Drücken*. Ph.D. thesis, Universität Hannover.

Schulze F., Behrens H., and Hurkuck W. (1999) Determination of the influence of pressure and dissolved water on viscosity of high viscous melts—Application of a new parallel-plate viscometer. *Am. Mineral.* **84,** 1512–1520.

Seki K. and Oeters F. (1984) Viscosity measurements on liquid slags in the system CaO-FeO-Fe_2O_3-SiO_2. *T. Iron Steel I. Jpn.* **24,** 445–454.

Shaw H. R. (1963) Obsidian-H_2O viscosities at 100 and 200 bars in the temperature range 700 to 900°C. *J. Geophys. Res.* **68,** 6337–6342.

Stevenson R. J., Dingwell D. B., Bagdassarov N. S., and Manley C. R. (2001) Measurement and implication of "effective" viscosity for rhyolite flow emplacement. *B. Volcanol.* **63,** 227–237.

Taniguchi H. (1993) On the volume dependence of viscosity of some magmatic silicate melts. *Mineral. Petrol.* **49,** 13–25.

Taniguchi H. and Murase T. (1987) Some physical properties and melt structures in the system diopside-anorthite. *J. Volcanol. Geotherm. Res.* **34,** 51–64.

Toguri J. M., Kaiura G. H., Marchant G. (1976) The viscosity of the molten FeO-Fe_2O_3-SiO_2 system. In *Extractive Metallurgy of Copper I*, pp. 259–273. Metallurgical Society of AIME.

Urbain G., Bottinga Y., and Richet P. (1982) Viscosity of liquid silica, silicates and alumino-silicates. *Geochim. Cosmochim. Acta* **46,** 1061–1072.

Virgo D. and Mysen B. O. (1985) The structural state of iron in oxidized vs. reduced glasses at 1 atm: A ^{57}Fe Mössbauer study. *Phys. Chem. Miner.* **12,** 65–76.

Wang Z., Cooney T. F., and Sharma S. K. (1995) In situ structural invesitagtion of iron-containing silicate liquids and glasses. *Geochim. Cosmochim. Acta* **59,** 1571–1577.

Waychunes G. A., Brown G. E. J., and Ponader C. W. (1988) Evidence from X-ray absorption for network-forming Fe^{2+} in molten alkali silicates. *Nature* **332,** 251–253.

Webb S. L. and Dingwell D. B. (1990) Non-Newtonian rheology of igneous melts at high sresses and strain rates: Experimental results for rhyolite, andesite, basalt and nephelinite. *J. Geophys. Res.* **95,** 15695–15701.

Whittington A., Richet P., and Holtz F. (2000) Water and the viscosity of depolymerized aluminosilicate melts. *Geochim. Cosmochim. Acta* **64,** 3725–3736.

Whittington A., Richet P., Linnard Y., and Holtz F. (2001) The viscosity of hydrous phonolites and trachytes. *Chem. Geol.* **174,** 209–223.

Wilke M., Behrens H., Burkhard D. J. M., and Farges F. (2002) The redox state of iron in depolymerized silicate melt at 500 MPa water pressure. *Chem. Geol.*, **189,** 55–67.

Williamson J., Tipple A. J., and Rogers P. S. (1968) Influence of iron oxides on kinetics of crystal growth in CaO-MgO-Al_2O_3-SiO_2 glasses. *J. Iron Steel I.* **206,** 898–903.

Wilson A. D. (1960) The micro-determination of ferrous iron in silicate minerals by a volumetric and a colormetric method. *Analyst* **85,** 823–827.

Zhang Y. X., Xu Z. J., and Behrens H. (2000) Hydrous species geospeedometer in rhyolite: Improved calibration and application. *Geochim. Cosmochim. Acta* **64,** 3347–3355.